Investigation of phase relationships and physical properties of Yb–Pd–Ge compounds

Yu.D. Seropegin, O.L. Borisenko, O.I. Bodak, V.N. Nikiforov, M.V. Kovachikova, Yu.V. Kochetkov

Chemistry Department, M.V. Lomonosov Moscow State University, 119899 Moscow, GSP-3, Leninskie Gory, Russia

Abstract

A variety of physicochemical analysis techniques were employed in constructing the isothermal cross-section of the phase diagram of the Yb–Pd–Ge system 870 K. Several new ternary compounds $Yb_{10}Pd_{75}Ge_{15}$, $Yb_{20}Pd_{20}Ge_{60}$, Yb_2PdGe_6, $YbPdGe_2$, $YbPd_2Ge$, $YbPdGe$, $YbPd_{0.5}Ge_{1.5}$, $Yb_{33.3}Pd_{28}Ge_{38.7}$ and $Yb_{42}Pd_{13}Ge_{45}$ were detected. The temperature dependences of the specific electric resistance were investigated for the alloys on the basis of $YbPdGe$, $YbPd_2Ge$ and $YbPd_2Ge_2$ compounds as well as for $Yb(PdGe)_3$ (alloy from the range of solid solutions based on $YbPd_3$).

Keywords: Phase relationships; Physical properties; Physicochemical analysis techniques

The aim of the present work was to study the phase equilibria in the Yb–Pd–Ge system, the form of the isothermal section at 870 K, synthesis of new ternary intermetallics and determination of their crystal structures.

Up to now there have been no data about the physical-chemical interaction of the components in the Yb–Pd–Ge system in the literature. Only one of the compounds of this system has been described, namely $YbPd_2Ge_2$ [1] with the $CeCa_2Al_2$ type ($ThCu_2Si_2$) structure and lattice parameters $a = 0.4287$ nm and $c = 1.0020$ nm. According to the data in [2], $YbPd_2Ge_2$ is a superconductor with a transition temperature of $T_c = 1.17$ K.

The binary systems Yb–Pd, Yb–Ge and Pd–Ge, forming the boundaries of the ternary system under investigation, have been studied in detail [3–11]. The crystallographic data of the corresponding binary compounds are listed in Table 1.

The phase equilibria in the Yb–Pd–Ge system have been studied by us on 152 samples. For the alloy preparation we used ytterbium (purity, 99.98%), palladium (purity, 99.99%) and germanium (purity, 99.99%). The alloys were prepared in an electric arc furnace in an atmosphere of purified argon. Homogenization annealing was performed in double quartz ampoules in an argon atmosphere at 870 K for 600 h

followed by quenching into ice–water. The alloy preparation was not free of difficulties because of the differences between temperatures of melting and boiling of the components and corresponding mass losses. After melting, the alloys were therefore weighed and only those having mass losses less than 1.5% were chosen for further investigation.

For the investigation of the samples obtained we used microstructural analysis, X-ray diffraction and local X-ray spectral analysis. We also studied the dependence of the specific electric resistance on temperature and investigated some magnetic properties.

Microstructural analysis was done on a Neophot 32 microscope after electrolytic etching of the samples with the use of nitric acid and hydrochloric acid in a ratio 3:1.

X-ray phase analysis was carried out on powder samples (RKD-57 cameras; Cr Kα irradiation).

Structural analysis was performed by X-ray powder diffraction (DRON-2; Fe Kα irradiation) (DRON-3; Cu Kα irradiation).

Local X-ray spectral analysis was done on the Camebax microbeam microanalyzer using the Lα lines for Yb, Pd and Ge. Numerical evaluation of the results was carried out by standard computer programs.

The temperature dependence of the specific electric resistance $\rho(T)$ was investigated at low temperatures

Table 1
Crystal data for the binary alloy systems Yb–Pd, Yb–Ge and Pd–Ge

Compound	Structure type	Space group	Lattice parameters				Reference
			a (nm)	b (nm)	c (nm)	β (°)	
α-Yb$_3$Ge$_5$	Th$_3$Pd$_5$	$P\bar{6}2m$	0.6847		0.4176		[3]
β-Yb$_3$Ge$_5$							[3]
Yb$_{11}$Ge$_{10}$	Ho$_{11}$Ge$_{10}$	$I4mmm$	1.072		1.653		[3]
Yb$_5$Ge$_3$	Mn$_5$Si$_3$	$P6_3/mcm$	0.8350		0.6407		[3]
YbPd$_3$	AuCu$_3$	$Pm\bar{3}m$	0.4054				[4]
YbPd$_{2.13}$	–	–	–	–	–		[4]
YbPd$_2$	–	–	–	–	–		[4]
YbPd$_{1.63}$	–	–	–	–	–		[4]
Yb$_3$Pd$_4$	Pu$_3$Pd$_4$	$R\bar{3}$	1.2900		0.5654		[4]
β-YbPd	CsCl	$Pm\bar{3}m$	0.3447				[4]
α-YbPd	FeB	$Pnma$	0.7720	0.4123	0.5178		[4]
α-Yb$_5$Pd$_2$	Mn$_5$C$_2$	$C2/c$	1.6321	0.6550	0.7680	97.32	[4]
Yb$_3$Pd	Fe$_3$C	$Pnma$	0.7664	0.9678	0.6500		[4]
α-Pd$_5$Ge	Pd$_5$As	$C2$	0.5509	0.7725	0.8375	98.03	[5]
β-Pd$_5$Ge	W	$Im\bar{3}m$	0.3083				[6]
Pd$_{25}$Ge$_9$	Pd$_{25}$Ge$_9$	$P\bar{3}$	0.735		1.059		[7]
			0.735		1.060		[8]
Pd$_{21}$Ge$_8$	Pt$_8$Al$_{21}$	$I4_1/a$	1.305		1.002		[7]
			1.3067		1.0033		[9]
Pd$_2$Ge	Fe$_2$P	$P\bar{6}2m$	0.666		0.338		[10]
PdGe	MnP	$Pnma$	0.6253	0.5782	0.343		[11]

in the temperature range 4–200 K. Measurements were performed by a standard four-probe method using a.c. and constant-current techniques. A Solartron 7081 precision voltmeter and a Unipan lock-in nanovoltmeter were used. The sample temperature was measured with the help of a calibrated germanium temperature detector. The temperature change was produced by means of a vertical shift of the sample with the thermometer in a temperature gradient under the liquid-helium level. The relative uncertainty in the resistance determination was less than 0.1 K.

The magnetic properties of a number of the compounds obtained were studied with the help of a Park-135 vibrational magnetometer in the temperature range 6–300 K in magnetic flux densities up to 0.3 T.

On the basis of the results obtained, we constructed the isothermal section of the equilibrium diagram of Yb–Pd–Ge at 870 K, which is presented in Fig. 1.

The existence of the binary compounds listed in Table 1 except for Yb$_{11}$Ge$_{12}$ and Yb$_5$Ge$_3$ is confirmed. (However, the latter fact is not in conflict with literature data since the first compound in [2] was synthesized by powder metallurgy and is supposed to be stabilized by the oxygen impurities, whereas YbPd$_2$ exists in the temperature range above the temperature considered in our investigation [4].)

In the ternary system Yb–Pd–Ge we confirmed the existence of the compound YbPd$_2$Ge$_2$ with a
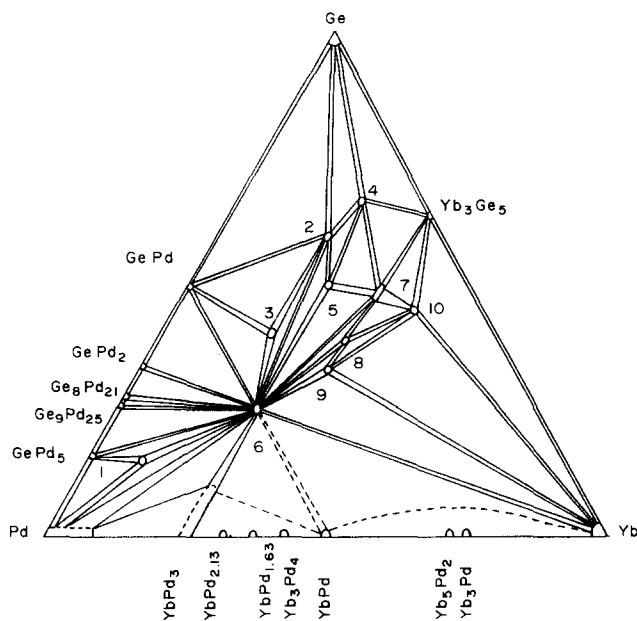

Fig. 1. Isothermal cross-section of the phase diagram of Yb–Pd–Ge system at 870 K: 1, Yb$_{10}$Pd$_{75}$Ge$_{15}$; 2, Yb$_{20}$Pd$_{20}$Ge$_{60}$; 3, YbPd$_2$Ge$_2$; 4, Yb$_2$PdGe$_6$; 5, YbPdGe$_5$; 6, YbPd$_2$Ge; 7, YbPd$_{0.5}$Ge$_{1.5}$; 8, Yb$_{33.3}$Pd$_{28}$Ge$_{38.7}$; 9, YbPdGe; 10, Yb$_{42}$Pd$_{13}$Ge$_{45}$.

CeCa$_2$Al$_2$ structure type ($a = 0.42841$ nm and $c = 1.0001$ nm).

The existence of nine new ternary intermetallic compounds was established. Their crystallographic characteristics are given in Table 2.

Table 2
Crystal data for ternary Yb–Pd–Ge alloys

Compound	Structure type	Space group	Lattice parameters (nm)		
			a	b	c
1 $Yb_{10}Pd_{75}Ge_{15}$	–	–	–	–	–
2 $Yb_{20}Pd_{20}Ge_{60}$	–	–	–	–	–
3 $YbPd_2Ge_2$	$CeCa_2Al_2$	$I4/mmm$	0.42841(8)		1.0001(3)
4 Yb_2PdGe_6	Ce_2CuGe_6	$Amm2$	0.3974(7)	2.1834(2)	0.40689(6)
5 $YbPdGe_2$	$YIrGe_2$	$Immm$	0.4336(2)	0.8626(3)	1.6071(6)
6 $YbPd_2Ge$	–	–	–	–	–
7 $YbPd_{0.5}Ge_{1.5}$	AlB_2	$P6/mmm$	0.42276(3)		0.40686(6)
$YbPd_{0.62}Ge_{1.38}$			0.42263(1)		0.40649(1)
8 $Yb_{33.3}Pd_{28}Ge_{38.7}$	–	–	–	–	–
9 $YbPdGe$	KHg_2	$Imma$	0.4344(3)	0.6839(2)	0.7522(3)
10 $Yb_{42}Pd_{13}Ge_{45}$	–	–	–	–	–

The binary compounds of the Pd–Ge system almost do not dissolve ytterbium. The extent of ternary solid solutions of the other binary compounds does not exceed 2–4 at.% of the third component, excluding the range of solid solutions of Pd_3Yb which can accommodate 10 at.% Ge. The solid solution ranges of the rest of the compounds are small and do not exceed 2–3 at.% of either component. In the range from 25 to 100 at.% of Yb and from 0 to 10 at.% Ge the equilibria are indicated in Fig. 1 by broken lines. The reason for this is the presence of the large number of alloys with phase separation.

In Table 3 the data from local X-ray spectral analysis of a number of alloys are presented.

The temperature dependences of the specific electric resistance were investigated for the compounds Yb-PdGe, $YbPd_2Ge$ and $YbPd_2Ge_2$ as well as for $Yb_{25}Pd_{65}Ge_{10}$ ($Yb(Pd_{1-x}Ge_x)_3$, solid solution range of $YbPd_3$).

For YbPdGe (structure type, KHg_2) a drastic decrease in the specific electric resistance is observed in the $\rho(T)$ dependence up to 35% in the range 4.2–200 K (Fig. 2). It was shown from measurements of the temperature and field dependences of the magnetic moment M (Fig. 3) that the above-mentioned anomaly is related to a ferromagnetic phase transition. The hysteresis on the curve M(H) was detected below T_c^*, the temperature of the magnetic ordering.

Table 3
Data of local X-ray spectral analysis on Yb–Pd–Ge alloy systems

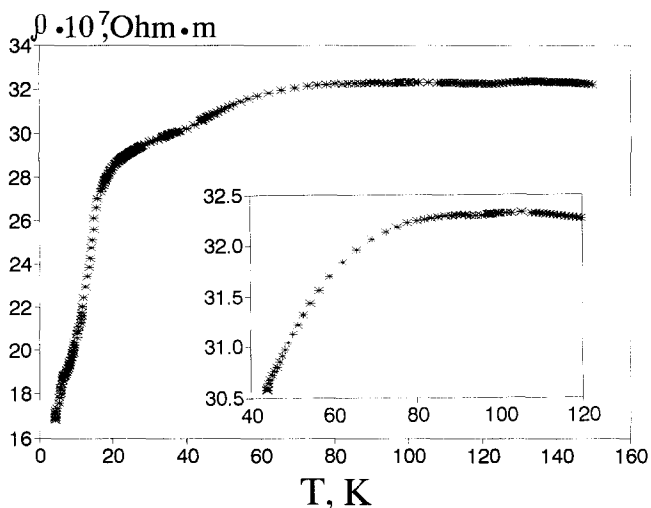| Composition (at.%)	Number of phases	Composition (at.%)			Phase
		Yb	Pd	Ge	
$Yb_{33.3}Pd_{33.3}Ge_{33.4}$	1	34.19	33.97	31.83	YbPdGe
		34.16	34.89	30.96	
		33.50	34.53	31.97	
		35.52	33.78	30.69	
		33.80	35.70	30.49	
		34.79	34.68	30.53	
$Yb_{33.3}Pd_{28}Ge_{38.7}$	1	34.69	27.69	37.63	$Yb_{33.3}Pd_{28}Ge_{38.7}$
		35.97	26.32	37.71	
		34.96	28.12	36.92	
		35.53	28.13	36.34	
$Yb_{42}Pd_{13}Ge_{45}$	1	44.23	12.35	43.42	$Yb_{42}Pd_{13}Ge_{45}$
		41.93	13.93	44.40	
		41.05	13.41	45.55	
		41.62	11.38	47.00	
$Yb_{33.3}Pd_{20.7}Ge_{46}$	1	35.37	18.18	46.44	$YbPd_{0.62}Ge_{1.38}$
		35.44	17.91	46.65	
		35.83	18.04	46.13	
		35.48	17.41	47.11	
		34.95	18.40	46.65	
$Yb_{25}Pd_{50}Ge_{25}$	1	27.53	49.07	23.41	$YbPd_2Ge$
		28.07	49.59	22.34	

Fig. 2. Temperature dependence of the electrical resistivity $\rho(T)$ of YbPdGe.
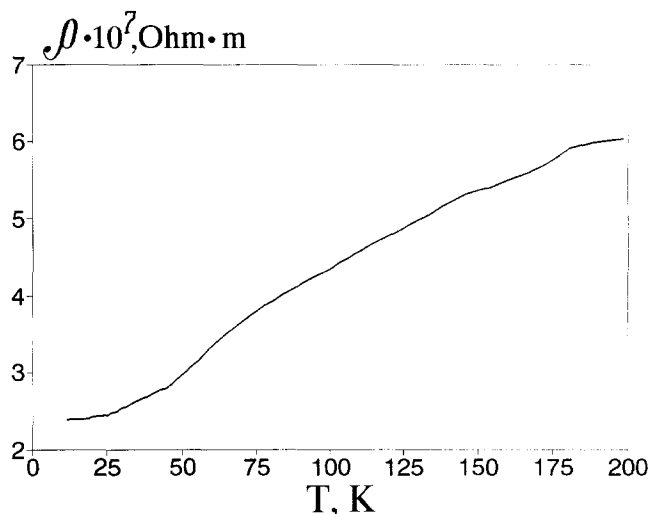

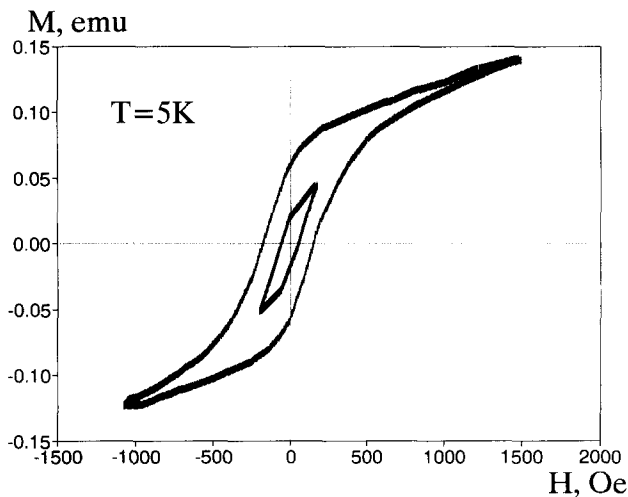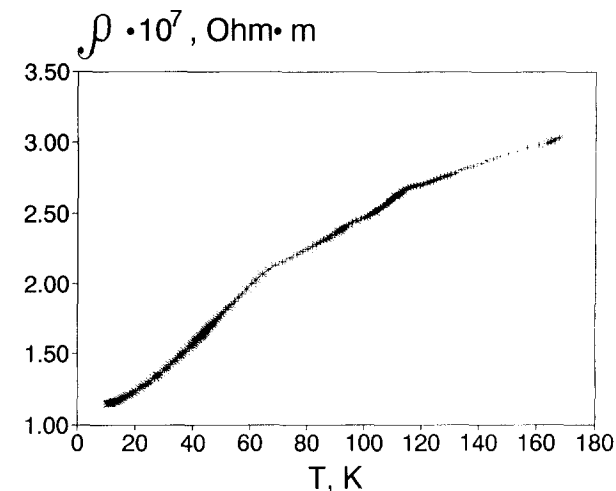Fig. 4. Temperature dependence of the electrical resistivity $\rho(T)$ of YbPd$_2$Ge.

Fig. 3. Magnetization curve at $T \approx 5$ K of YbPdGe.

Fig. 5. Temperature dependence of the electrical resistivity $\rho(T)$ of YbPd$_2$Ge$_2$.

YbPd$_2$Ge (structure type not established) demonstrates the usual metallic decrease in the specific electric resistance dependence on temperature with saturation at low temperatures (Fig. 4).

For YbPd$_2$Ge$_2$ (structure type, CeCa$_2$Al$_2$), in the $\rho(T)$ curve a deviation from linear behavior in the range 100–150 K was observed (Fig. 5). This allows us to suppose Kondo scattering of conduction electrons on the localized magnetic moments of Yb ions (by analogy with the recently investigated YbPd$_2$Si$_2$).

The $\rho(T)$ curves for YbPd$_2$Ge$_2$ and YbPd$_2$Ge were obtained in the temperature range 10–200 K. The temperature dependence of magnetic susceptibility in this interval demonstrates the usual Curie–Weiss law. The physical interpretation of the resistance behavior below 10 K needs additional experiments.

For Yb$_{25}$Pd$_{65}$Ge$_{10}$ (structure type, AuCu$_3$), an abrupt decrease in the specific electric resistance is observed

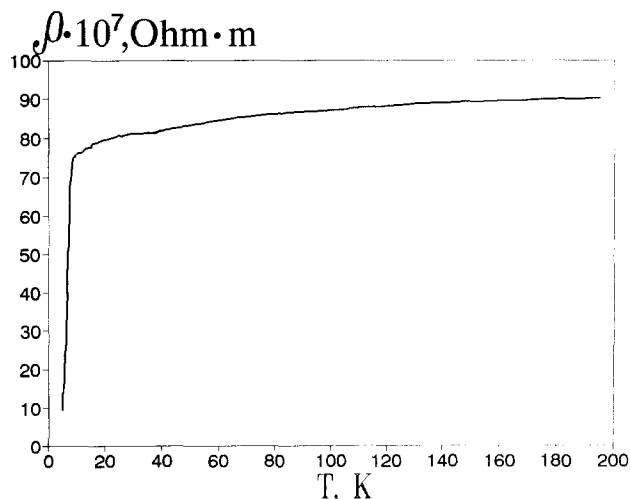Fig. 6. Temperature dependence of the electrical resistivity $\rho(T)$ of Yb(Pd$_{1-x}$Ge$_x$)$_3$.
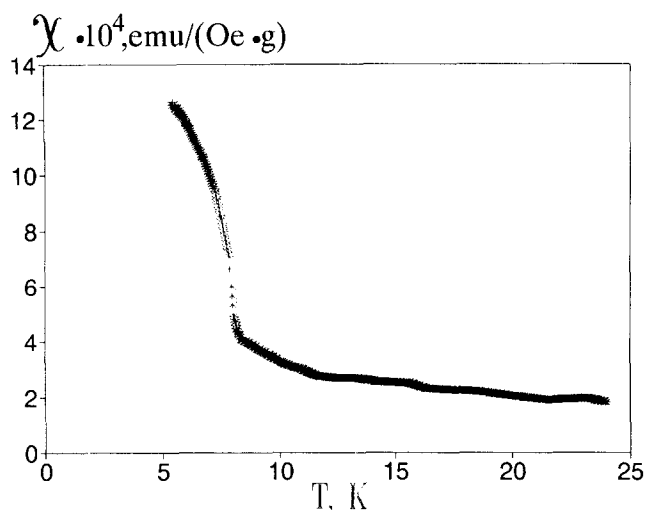
$\chi \cdot 10^4, \text{emu/(Oe} \cdot \text{g)}$

Fig. 7. Temperature dependence of the magnetic susceptibility of the $Yb(Pd_{1-x}Ge_x)_3$.

in the $\rho(T)$ dependence up to 80% below $T_c = 8$ K (Fig. 6).

The temperature dependence of magnetic susceptibility demonstrates the anomaly below this temperature T_c (Fig. 7).

References

[1] D. Rossi, R. Marazza and R. Ferro, *J. Less-Common Met.*, 66 (1979) 17.
[2] G.W. Hull, J.H. Wernick, T.H. Geballe, J.V. Waszczak and J.E. Bernardini, *Phys. Rev. B*, 24 (1981) 6715.
[3] B.N. Eremenko, K.A. Meleshevich and Yu.I. Bujanov, *Dokl. Akad. Nauk USSR, Ser. A*, 3 (1983) 84.
[4] A. Iandelli and A. Palenzona, *Rev. Chim. Minér.*, 10 (1973) 303.
[5] T. Matkovis and K. Schubert, *J. Less-Common Met.*, 58 (1978) 1.
[6] M. Ellner and B. Predel, *J. Less-Common Met.*, 76 (1980) 181.
[7] K. Khalaff and K. Schubert, *Z. Metallkd.*, 65 (1974) 379.
[8] W. Wopersnow and K. Schubert, *J. Less-Common Met.*, 41 (1975) 97.
[9] P. Matkovic, W. Wopersnow and K. Schubert, *J. Less-Common Met.*, 56 (1977) 69.
[10] K. Anderko and K. Schubert, *Z. Metallkd.*, 44 (1953) 307.
[11] E.J. Graeber, R.J. Baughoman and B. Morosin, *Acta Crystallogr.*, 29 (1973) 1991.